Springer

KSME

Journal of Mechanical Science and Technology 31 (9) (2017) 4159~4165
www.springerlink.com/content/1738-494x(Print)/1976-3824(Online)
DOI 10.1007/s12206-017-0812-y

Taguchi-based grey relational analysis for modeling and optimizing machining parameters through dry turning of Incoloy 800H †

Palanisamy Angappan[1,*], Selvaraj Thangiah[1] and Sivasankaran Subbarayan[2]

[1]Department of Production Engineering, National Institute of Technology, Tiruchirappalli-620 015, India
[2]Department of Mechanical Engineering, College of Engineering, Qassim University, Buraidah, Saudi Arabia

(Manuscript Received August 12, 2016; Revised April 18, 2017; Accepted May 24, 2017)

Abstract

The present research focused on the optimization of machining parameters and their effects by dry-turning an incoloy 800H on the basis of Taguchi-based grey relational analysis. Surface roughness (*Ra, Rq* and *Rz*), cutting force (*Fz*), and cutting power (*P*) were minimized, whereas Material removal rate (*MRR*) was maximized. An L_{27} orthogonal array was used in the experiments, which were conducted in a computerized and numerical-controlled turning machine. Cutting speed, feed rate, and cut depth were set as controllable machining variables, and analysis of variance was performed to determine the contribution of each variable. We then developed regression models, which ultimately conformed to investigational and predicted values. The combinational parameters for the multiperformance optimization were $V = 35$ m/min, $f = 0.06$ mm/rev and $a = 1$ mm, which altogether correspond to approximately 48.98 % of the improvement. The chip morphology of the incoloy 800H was also studied and reported.

Keywords: Dry turning; Incoloy 800H; Taguchi method; Regression; Optimization; Chip morphology

1. Introduction

In the aerospace industry, about 45 %-50 % of gas-turbine engines are composed of superalloys [1], such as Incoloy 800H, which is an austenitic Fe-Ni-Cr alloy (superalloy). Typical applications of incoloy 800H include the heat-exchanging components of conventional power and petrochemical plants, reheaters in power plants, superheaters, hot ducts, steam generator tubes in nuclear power plants, fuel claddings, and pressure vessels where operating temperature often ranges from 550 °C to 700 °C [2]. Superalloys are complicated materials for machining because of their rapid hardening and massive strength properties even at high temperatures, similarity to chipped materials along a cutting boundary, and low thermal conductivity [3, 4]. Nonetheless, Fe-Ni-Cr alloys are widely explored in the manufacturing sector because of their relatively better properties at high temperature compared with those of titanium alloys [5], although the force required to cut superalloys are nearly twice of that required to cut alloy steels. Moreover, Incoloy 800H also hardens easily while machining and thus has poor machinability. In the past, selection of machining parameters for these hard superalloys are based on knowledge, skills, and experience of operators, apart from referring to standard handbooks. However, selected machining input parameters are usually not optimized, thereby leading to low production rates [6]. Moreover, the surface roughness of machined components mainly depends on the material properties, especially fatigue strength and resistance to wear and corrosion [7, 8].

Studies that focused on the machining parameters of Incoloy 800H are extremely rare. Thus, in this work, the turning behavior and optimization of Incoloy 800H superalloy were studied through the use of uncoated carbide inserts. The main plots were determined, and Analysis of variance (ANOVA) was performed to identify the relation of machining variables with the responses for *Ra, Rq, Rz, Fz, P* and *MRR*. Taguchi-based analysis with grey-based approach was used to optimize the selected process parameters through the conversion of multiple responses into a single response [9-12].

2. Materials and methods

An Incoloy 800H superalloy with 120 mm length and 25 mm diameter was used for the experiments. Incoloy 800H (wt%) is chemically composed of 0.069 % C, 45.56 % Fe, 31.59 % Ni, 20.42 % Cr, 0.76 % Mn, 0.57 % Ti, 0.5 % Al, 0.42 % Cu, 0.13 % Si, 0.014 % P and 0.001 % S. Dry turning operations were performed in a computerized and numerical-

*Corresponding author. Tel.: +91 9994561450
E-mail address: palasamy1111@gmail.com (A. Palanisamy), tselva@nitt.edu (T. Selvaraj), sivasankarangs1979@gmail.com, s.udayar@qu.edu (S. Sivasankaran)
† Recommended by Associate Editor Sang-Hee Yoon

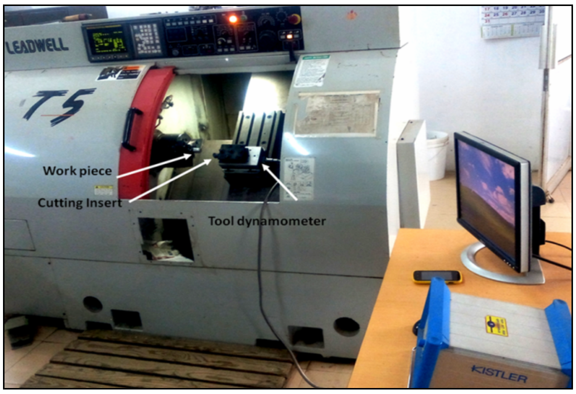

Fig. 1. Experimental setup.

controlled Leadwell turning machine with 4500 rpm capacity and 7.5 kW power. The experimental is shown in Fig. 1. An *ISO*-labeled *PCLNL 1610 M12* tool holder and *CNMA 120408-THM (WIDIA-India)* uncoated tungsten carbide inserts were applied with the following tool geometries: (i) Clearance angle = 5°, (ii) side rake angle = -6°, (iii) inclination angle = -6°, (iv) approach angle = 95°, (v) point angle = 80° and (vi) nose radius = 0.8 mm. For the experimental design, the first, second, and fifth columns of the L_{27} (3^{13}) standard Orthogonal array (*OA)* were set with the following measurements: Cutting speed (V = A; 35, 35 and 55 m/min), feed rate (f = B; 0.02, 0.04 and 0.06 mm/rev), and cut depth (a = C; 0.5, 0.75 and 1 mm) according to the linear graph. A Mitutoyo surftest (SJ-310; cutoff length = 0.8 mm, traverse length = 5 mm) was used to measure the roughness of the machined surfaces. The cutting force was recorded by a piezoelectric dynamometer (Kistler type 9257B). Finally, *power* and *MRR* were determined by their standard formulas. The experimental results are shown in Table 1.

Table 1. Experimental results.

Ex. No.	Experimental results					
	Ra (μm)	*Rq* (μm)	*Rz* (μm)	*Fz* (N)	*Power* (W)	*MRR* (mm^3/sec)
1	1.29	1.75	9.52	171.9	6016.5	5.83
2	1.29	1.77	9.07	181.1	6336.9	8.75
3	1.36	1.77	8.81	193.6	6774.6	11.67
4	1.42	1.88	10.71	175.9	6157.6	11.67
5	1.45	1.88	10.42	184.2	6447	17.50
6	1.48	1.89	9.99	195.4	6839	23.33
7	1.59	1.99	11.70	179.4	6278	17.50
8	1.62	2.01	11.44	186.4	6524	26.25
9	1.61	2.02	10.92	197.5	6912.5	35.00
10	1.26	1.70	7.98	167.5	7538	7.50
11	1.29	1.73	7.69	176.9	7961	11.25
12	1.27	1.70	7.21	183.9	8275.1	15.00
13	1.34	1.87	8.99	165.7	7456.5	15.00
14	1.42	1.90	8.69	178.1	8014.2	22.50
15	1.44	1.88	8.51	184.7	8310.3	30.00
16	1.48	2.03	10.37	169.4	7624.4	22.50
17	1.56	1.99	9.88	178.6	8036.6	33.75
18	1.55	2.01	9.56	182.7	8220.1	45.00
19	1.19	1.69	6.52	154.9	8519.5	9.17
20	1.21	1.72	6.24	159.0	8747.1	13.75
21	1.24	1.71	5.75	172.6	9490.1	18.33
22	1.29	1.86	7.66	155.6	8558.2	18.33
23	1.34	1.86	7.41	159.9	8792.9	27.50
24	1.35	1.87	7.18	175.5	9652.5	36.67
25	1.46	2.00	9.02	151.8	8351	27.50
26	1.51	2.01	8.73	163.0	8962.3	41.25
27	1.51	1.98	8.36	171.1	9409.4	55.00

3. Analysis of experimental data

3.1 Signal-to-noise (S/N) analysis

Taguchi with Grey relational analysis (GRA) can be used to determine the optimization of multiple performance characteristics. Compared with conventional results, the smaller/higher and better quality attributes can be determined by Eqs. (1) and (2), respectively.

$$\text{S/N ratio } (\eta) = -10\text{xLog}\,[1/n\ \text{x}((Y_1)^2+(Y_2)^2+\text{--}+(Y_n)^2)] \quad (1)$$

$$\text{S/N ratio } (\eta) = -10\text{xLog}\,[1/n\ \text{x}\,((1/Y_1)^2+\text{---}+(1/Y_n)^2)] \quad (2)$$

where Y_1, $Y_2 \ldots Y_n$ are the responses taken separately for the trail condition, which recur n times. The S/N ratios from the above equations and their mean values are shown in Table 2.

3.2 Grey relational analysis

GRAs are conducted to analyze the performance of unidentifiable methods [10], while Grey relational grades (GRG) with weighting factors are established to obtain machining responses. The grey relations and their equivalent normalized data can be expressed as follows:

For the Smaller-the-better (SB) condition,

$$x_i(k) = \frac{\max y_i(k) - y_i(k)}{\max y_i(k) - \min y_i(k)} \quad (3)$$

For the Larger-the-better (LB) condition,

$$x_i(k) = \frac{y_i(k)) - \min y_i(k)}{\max y_i(k) - \min y_i(k)} \quad (4)$$

where $x_i(k)$ is the value after the grey relational generation, and min $y_i(k)$ and max $y_i(k)$ are the smallest and largest values of $y_i(k)$ for the k^{th} performance. The GRG in the GRA explains the relational degree of the 27 sequences of $[x0(k)$ and $x_i(k)$, i =1,2,…27; k =1,2,….,27]. However, before completing the GRG, the Grey relational coefficient

Table 2. Mean values of the S/N ratio.

(a)	S/N ratio for *Ra*		
	Total S/N mean = -2.8891		
	Level 1	Level 2	Level 3
V	-3.2310	-2.0467	-2.6850
f	-2.9029	-2.8642	-2.9475
a	-2.5334	-3.7564	-3.0347
Optimal parameters: A3B1C1			
(b)	S/N ratio for *Rq*		
	Total S/N mean = -5.4083		
	Level 1	Level 2	Level 3
V	-5.4865	-4.7373	-5.3845
f	-5.4010	-5.4536	-5.4262
a	-5.3375	-6.0341	-5.4142
Optimal parameters: A3B1C1			
(c)	S/N ratio for *Rz*		
	Total S/N mean = -18.7782		
	Level 1	Level 2	Level 3
V	-20.207	-17.546	-19.116
f	-18.800	-18.845	-18.800
a	-17.327	-19.943	-18.419
Optimal parameters: A3B1C3			
(d)	S/N ratio for *Fz*		
	Total S/N mean = -44.8234		
	Level 1	Level 2	Level 3
V	-45.336	-44.766	-44.378
f	-44.923	-44.840	-44.803
a	-44.211	-44.864	-45.290
Optimal parameters: A3B1C1			
(e)	S/N ratio for *Power*		
	Total S/N mean = -77.7410		
	Level 1	Level 2	Level 3
V	-76.217	-77.684	-77.296
f	-77.987	-77.758	-77.720
a	-79.019	-77.782	-78.207
Optimal parameters: A1B1C1			
(f)	S/N ratio for *MRR*		
	Total S/N mean = -25.7231		
	Level 1	Level 2	Level 3
V	23.6868	20.5354	22.542
f	25.8697	26.5560	26.064
a	27.6127	30.0778	28.562
Optimal parameters: A3B3C3			

(GRC) should be obtained. The GRC $\xi i(k)$ can be expressed as

$$\xi i(k) = \frac{\Delta\min + \xi\Delta\max}{\Delta 0i + \xi\Delta\max} \tag{5}$$

Table 3. Grey relational grade and rank.

Ex. No.	*Grade*	*Rank*
1	0.429	25
2	0.454	23
3	0.518	17
4	0.531	15
5	0.565	13
6	0.629	9
7	0.688	6
8	0.749	3
9	0.811	1
10	0.416	26
11	0.455	22
12	0.479	21
13	0.485	19
14	0.556	14
15	0.593	12
16	0.771	2
17	0.686	7
18	0.730	4
19	0.406	27
20	0.432	24
21	0.497	18
22	0.481	20
23	0.519	16
24	0.610	10
25	0.596	11
26	0.678	8
27	0.725	5

where $\Delta oi = \|x0(k) - xi(k)\|$ is the difference of the absolute value between $x0(k)$ and $x_i(k)$, while ξ is the distinguishing coefficient, which is assumed as 0.5. Moreover, $\Delta\min = \forall j \min \in i \forall k \min \|x0(k) - xj(k)\|$ equals to the smallest value of $\Delta 0i$, while $\Delta\max = \forall j \max \in i \forall k \max \|xo(k) - xj(k)\|$ equals to the largest value of $\Delta 0i$. Furthermore,

$$\gamma i = \frac{1}{n} \sum_{k=1}^{n} \xi i(k) \tag{6}$$

where n is the number of responses, in which the weights are assigned by the following state:

$$\sum_i^n wi = 1 . \tag{7}$$

A large GRG indicates good multiple response characteristics. In the present study, the ninth experiment obtained the

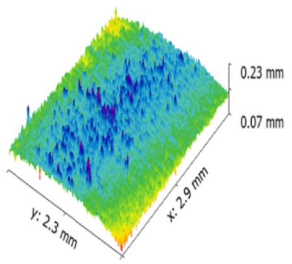

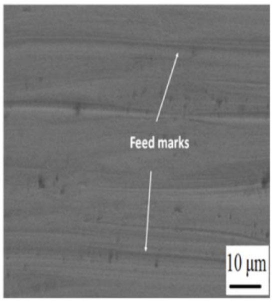

(a) (b)

Fig. 2. (a) 3D surface profile; (b) SEM image.

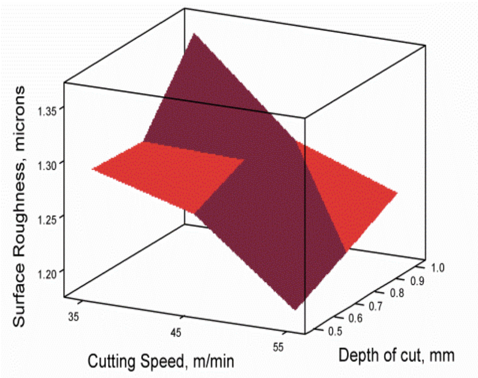

Fig. 3. Surface roughness at f = 0.02 for varying V and a.

largest GRG value. The best optimum combinational parameters were ***A1B3C3***, as shown in Table 3.

4. Results and discussions

4.1 Effect of machining variables on surface roughness

The values of the surface roughness parameters (*Ra, Rq* and *Rz)* were measured on three machined surface locations at each experimental run. The average values were then calculated. Surface roughness intensified as feed rate increased from 0.02 mm/rev to 0.06 mm/rev, further resulting in an increase in *MRR* at definite speeds [11]. For optimal combinational conditions, the values of *Ra, Rq* and *Rz* were 1.61, 2.02 and 10.923 µm, respectively. Fig. 2(a) shows the 3D profile of the surface roughness. The profile was obtained using a high-resolution white light interferometer and scanning electron microscopic image of the machined sample corresponding to an optimal condition. Fig. 3 shows the effect of surface roughness at a low feed rate of 0.02 mm/rev. Furthermore, the surface roughness value decreased when the cutting speed increased. By contrast, the surface roughness value increased when the cut depth increased. The obtained surface roughness value in this study (1.35 µm) was higher than previously reported values and was obtained at a low cutting speed (35 m/min) and high cut depth (1 mm). Furthermore, a low surface roughness of 1.18 µm was obtained at the highest cutting speed (55 m/min), lowest cut depth (0.5 mm), and low feed rate (0.02 mm/rev). These values can be attributed to the low amount of material ploughing and low feed rates. The thickness of uncut chips were small at low feed rates, and this condition can diminish ploughing and result in a good surface roughness. However, as the feed rate increased, the ploughing effect also increased, subsequently resulting in a poor surface finish.

4.2 Effect of machining variables on cutting force (F_Z)

Cutting force gradually increased when the feed rate increased, and this condition was attributed to the strain hardening effect produced by severe plastic deformations during the metal cutting process. As the feed rate increased, the quantity of materials that were in contact with the cutting tool also increased. Furthermore, the value of cutting force increased at increased tool-work contact length. The optimal cutting force (*Fz*) was 197.50 N, a value obtained at f = 0.06 mm/rev, a = 1 mm and V = 35 m/min. The value of the cutting force decreased when the cutting speed increased from 35 m/min to 55 m/min because of thermal softening that occurred in the sample. However, the cut depth, along with the width of chips, increased, thereby increasing the cutting force.

4.3 Effect of machining variables on cutting power (P)

The consumed cutting power during machining is at the minimum for the low variable values. Cutting power was determined by multiplying cutting force (*Fz*) with cutting velocity (V). Heat generation at the interface between the tool and work piece increased when the cut depth increased, implying a high *MRR* value. Thus, the system required additional power. The highest obtained power was 9652.5 W during the 24th experiment with V = 55 m/min, a =1 mm and Fz = 175.50 N.

4.4 Effect of machining variables on MRR

The production rate during machining mainly depends on its *MRR*

$$MRR=V*f*a*1000/60 \text{ mm}^3/\text{sec} \tag{8}$$

where *MRR* is computed by mm^3/sec. The highest *MRR* was 55 mm^3/sec, which was obtained at the highest levels of inputs because of the high volume of materials removed.

4.5 Regression equations

MINITAB 16 software was used to develop linear regression models from the experimental outcome for the prediction of the responses. The following outcomes were obtained for the correlations and process variables:

$$Ra=1.29316-0.00560556*V+6.88611*f+0.111778*a \tag{9}$$

$$Rq=1.65042-0.00154297*V+6.94114*f+0.0117607*a \tag{10}$$

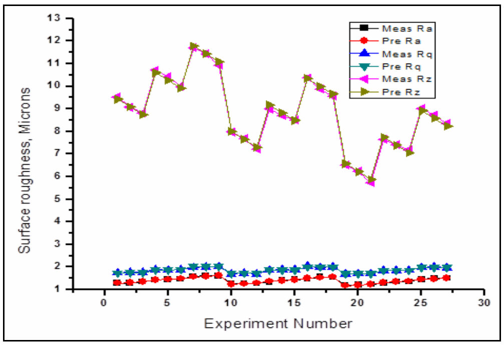

(a)

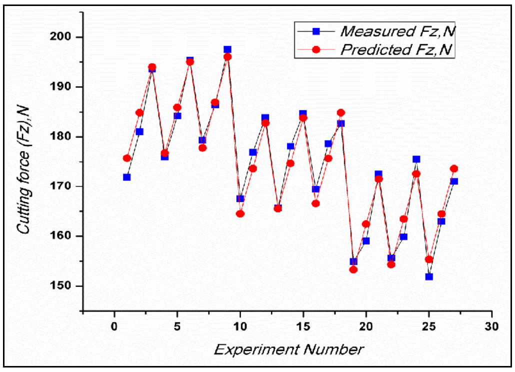

(b)

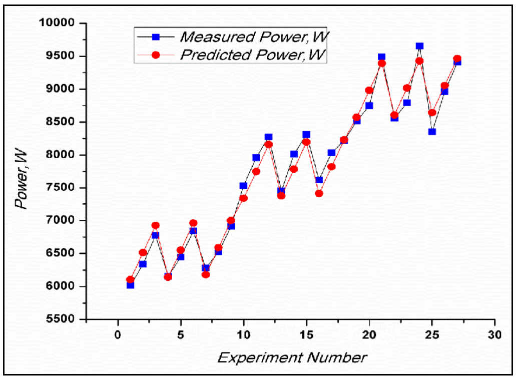

(c)

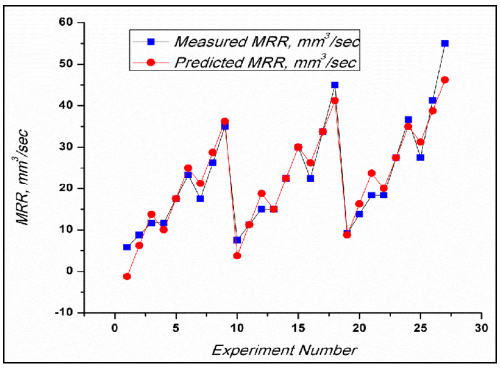

(d)

Fig. 4. (a) Experimental versus predicted values for *Ra, Rq* and *Rz*; (b) experimental versus predicted values for *Fz*; (c) experimental versus predicted values for *P*; (d) experimental versus predicted values for *MRR*.

Table 4. ANOVA of the performance characteristics of the responses.

Source	*DF*	*Adj SS*	*Adj MS*	*F-value*	*P-value*	*PC %*
(a) ANOVA analysis for *Ra*						
V	2	0.0566	0.0283	73.39	0.000	13.4
f	2	0.3424	0.1712	444.1	0.000	81.1
a	2	0.0154	0.0077	19.92	0.000	3.63
Error	20	0.0078	0.0004			1.83
Total	26	0.4219				100
(b) ANOVA analysis for *Rq*						
V	2	0.0043	0.0022	7.01	0.005	1.20
f	2	0.3474	0.1738	566.9	0.000	96.9
a	2	0.0003	0.0002	0.52	0.604	0.09
Error	20	0.0062	0.0004			1.71
Total	26	0.3582				100
(c) ANOVA analysis for *Rz*						
V	2	36.787	18.393	1706.1	0.000	57.3
f	2	24.975	12.488	1158.3	0.000	38.9
a	2	2.133	1.066	98.91	0.000	3.33
Error	20	0.216	0.011			0.33
Total	26	64.110				100
(d) ANOVA analysis for *Fz*						
V	2	2306.3	1153.1	216.59	0.000	58.4
f	2	20.49	10.24	1.92	0.172	0.51
a	2	1509.9	754.97	141.81	0.000	38.2
Error	20	106.48	5.32			2.7
Total	26	3943.2				100
(e) ANOVA analysis for *Power*						
V	2	276844	138422	877.3	0.000	89.1
f	2	28423	14212	0.90	0.422	0.09
a	2	30393	151961	96.32	0.000	9.78
Error	20	315546	15777			0.10
Total	26	310677				100
(f) ANOVA analysis for *MRR*						
V	2	450.00	225.00	15.92	0.000	11.1
f	2	2278.1	1139.0	80.60	0.000	56.6
a	2	1012.5	506.25	35.82	0.000	25.1
Error	20	282.64	14.13			7.02
Total	26	4023.2				100

$$Rz=13.932-0.142857*V+58.8935*f-1.37593*a \quad (11)$$
$$Fz=195.67-1.12214*V+51.4361*f+36.5864*a \quad (12)$$
$$P=932.164+123.317*V+1831.96*f+1640.89*a \quad (13)$$
$$MRR=-45+0.5*V+562.5*f+30*a. \quad (14)$$

Figs. 4(a)-(d) show the experimental values compared with the predicted values. Table 4 presents the ANOVA for *Ra, Rq, Rz, Fz, P* and *MRR* based on the mean values of the S/N response ratio. In addition, ANOVA was used to analyze the influence of the controllable factors on the responses at 5 %

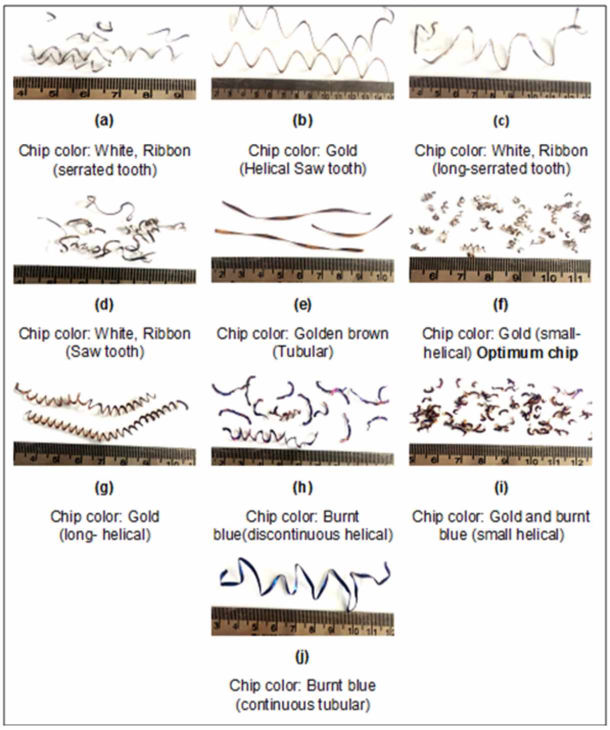

Fig. 5. Chips produced while turning the incoloy 800H.

significance level (i.e., 95 % confidence level based on *F*-value and *P*-value). A P-value of < 0.05 means that the factors have high influence on the responses.

4.6 Study of chip morphology

The color and shape of the chips were examined with a digital camera. The characteristics of the chip-tool interface affected by the uncoated carbide tools are shown in Figs. 5(a)-(j), which also correspond to experiment numbers 1, 5, 10, 15, 20, 9, 23, 25, 19 and 27. Rubbing in the tool and chip interface was one of the major factors that affected chip morphology. Curled chips were produced with a large diameter due to high friction on the contact surfaces during the turning of the incoloy 800H.

4.7 Confirmation experiments

The confirmation experiments were conducted three times to verify the accuracy of the optimization at optimal levels. The results are presented in Table 5. The GRG improved by 0.412 with percentage improvement of 48.98 %.

5. Conclusions

The optimum machining parameters obtained through the Taguchi method (i.e., based on responses and S/N ratio) for surface roughness *(Ra, Rq* and *Rz)*, cutting force *(Fz)*, power *(P)*, and *MRR* were ***A3B1C1, A3B1C1, A3B1C3, A3B1C1, A1B1C1*** and ***A3B3C3***, respectively.

Table 5. Results of the confirmation experiment.

	Initial condition	Optimal conditions	
		Prediction	Experiment
Levels	***A1B1C1***	***A1B3C3***	***A1B3C3***
Ra, μm	1.29		1.53
Rq, μm	1.750		1.951
Rz, μm	9.517		8.420
Fz, N	171.90		173.6
Power, W	6016.5		9548
MRR, mm^3/sec	5.83		55
GRG	0.429	0.811	0.841

Obtained through the Taguchi-based grey relational analysis, the optimum combinational parameter for the multiple responses was ***A1B3C3*** *(V* = 35 m/min*, f* = 0.06 mm/rev and *a* = 1 mm).

Regression models were developed for the responses, and the corresponding outcomes showed high conformity with the measurements for the predicted values, that is, R^2 values for *Ra, Rq, Rz, Fz*, *P* and *MRR* at 97.65 %, 98.09 %, 99.57 %, 96.15 %, 97.93 and 92.97, respectively.

As indicated by the ANOVA results, the most significant variable for the multiple response optimization is feed rate, as opposed to cutting speed and cut depth. The percentage contribution of feed rate was 81.20 %, which was noticeably higher compared with cutting speed (1.32 %), cut depth (9.15 %), and square term of feed rate (1.67 %).

Furthermore, in relation to the total effect based on the GRG, the contributed interaction effect of the cutting speed/feed rate was 1.113 %; cutting speed/cut depth, 1.21 %; and feed rate/depth of cut, 0.38 %. For the *MRR*, the contributed interaction of cutting speed/feed rate was 1.86 %, cutting speed/cut depth of cut was 0.82 %, and feed rate/cut depth was 4.19 %. For the cutting force, the contributed interaction effect of cutting speed/cut depth was 1.005 %. The interaction effects of all these factors (except feed rate/cut depth) were < 1.5 %, indicating nonsignificant relationship to total variation.

References

[1] K. Venkatesan, R. Ramanujam and P. Kuppan, Parametric modeling and optimization of laser scanning parameters during laser assisted machining of Inconel 718, *Optics & Laser Technology*, 78 (2016) 10-18.

[2] W. Ren and R. Swindeman, Status of Alloy 800 H in considerations for the Gen IV nuclear energy systems, *Journal of Pressure Vessel Technology*, 136 (5) (2014) 54001.

[3] D. Ulutan and T. Ozel, Machining induced surface integrity in titanium and nickel alloys: A review, *International Journal of Machine Tools and Manufacture*, 1 (3) (2011) 250-280.

[4] Y. B. Guo, W. Li and I. S. Jawahir, Surface integrity charac-

terization and prediction in machining of hardened and difficult-to-machine alloys: a state-of-art research review and analysis, *Machining Science and Technology*, 13 (4) (2009) 437-470.
[5] B. Davoodi and B. Eskandari, Tool wear mechanisms and multi-response optimization of tool life and volume of material removed in turning of N-155 iron-nickel-base superalloy using RSM, *Measurement*, 68 (2015) 286-294.
[6] D. Thakur, B. Ramamoorthy and L. Vijayaraghavan, Optimization of high speed turning parameters of superalloy Inconel 718 material using Taguchi technique, *Indian Journal of Engineering and Materials Sciences*, 16 (2009) 44-50.
[7] D. Singh and P. V. Rao, A surface roughness prediction model for hard turning process, *The International Journal of Advanced Manufacturing Technology*, 32 (11-12) (2007) 1115-1124.
[8] H. Ding and Y. C. Shin, Improving machinability of high chromium wear-resistant materials via laser-assisted machining, *Machining Science and Technology*, 17 (2) (2013) 246-269.
[9] A. S. Kuar, B. Acherjee, D. Ganguly and S. Mitra, Optimization of Nd: YAG laser parameters for microdrilling of alumina with multiquality characteristics via grey-Taguchi method, *Materials and Manufacturing Processes*, 27 (3) (2012) 329-336.
[10] L. Hsuan-Liang and Y. Jia-Ching, Optimization of weld bead geometry in the activated GMA welding process via a grey-based Taguchi method, *Journal of Mechanical Science and Technology*, 28 (8) (2014) 3249-3254.
[11] D. Palanisamy, P. Senthil and V. Senthilkumar, The effect of aging on machinability of 15Cr-5Ni precipitation hardened stainless steel, *Archives of Civil and Mechanical Engineering*, 16 (1) (2016) 53-63.
[12] R. K. Porwal, V. Yadava and J. Ramkumar, Modelling and multi-response optimization of hole sinking electrical discharge micromachining of titanium alloy thin sheet, *Journal of Mechanical Science and Technology*, 28 (2) (2014) 653-661.

Palanisamy Angappan completed his B.E. Mechanical Engineering from the University of Madras in 2000, and his Master of Technology in Manufacturing Technology in NIT, Tiruchirappalli, India in 2008. He worked as Assistant Professor in various engineering colleges in India for more than a decade. His current research interests are conventional and unconventional machining processes and optimization.